Cholesteric cellular patterns with electric-field-controlled line tension

O. D. Lavrentovich and D.-K. Yang

Chemical Physics Interdisciplinary Program and Liquid Crystal Institute, Kent State University, Kent, Ohio 44242

A field-induced instability of wall defects, commonly called oily streaks, is observed in cholesteric liquid crystals. The electric field favors reorientation of cholesteric layers and drives the line tension of the oily streaks negative. Defects with negative line tension elongate, preserving their width. The electrically controlled line tension is a nonmonotonic function of the width; streaks that are too narrow or too wide remain straight. The phenomenon is explained within a coarse-grain model that accounts for the surface anchoring. [S1063-651X(98)51006-9]

Soap froths, metallurgical, magnetic, and ceramic grain structures belong to a wide variety of random cellular structures whose patterns comprise edges that join vertices and surround faces [1]. These configurations are controlled by topological constraints and energy equilibrium of line (or surface) tensions. We describe a cellular pattern in which the line tension of edges is controlled by an applied electric field; the edges buckle and elongate when the field drives the line tension negative.

The experiments use cholesteric slabs bounded by glass plates with transparent electrodes. The cell thickness h is fixed in the range 5–25 μm by fiber spacers. The electrodes are coated with a polyimide layer to align the molecules in the plane of the plates. The effects described below depend very little on the type of in-plane anchoring (degenerate or uniaxial). We consider the case of degenerate anchoring (nonrubbed polyimide). When the field is absent ($\mathbf{E}=\mathbf{0}$) the slabs show a typical ''planar'' texture with uniform domains divided by oily streaks [Fig. 1(a)]. The oily streaks, known for more than a century [2], have the following features [3,4].

Within the uniform domains, the director $\mathbf{n}$ rotates in helicoidal fashion around an axis $\mathbf{m}$, with a pitch P. Since $\mathbf{n}(\mathbf{r})$ is periodic, one can define cholesteric ''layers'' parallel to the cell plates. Oily streaks are metastable defects provoked by inhomogeneities such as spacers. Inside the streak, the layers are bent as semicylinders and remain equidistant everywhere except the central wall. The bent layers form a pair of π disclinations separated by a distance $2a$ (Fig. 2). Inspection with a polarizing microscope confirms that the optic axis (the axis $\mathbf{m}$ in short-pitch materials) is normal to the streaks.

The cholesteric mixture is composed of two nematic materials EK1366718 and ZLI4330 (weight ratio 2:1) doped with chiral additives R811 and R1011 mixed at weight ratio 3:1. The weight concentration of the chiral dopant is between 5 and 15% (to change P between 1 and 0.3 μm). The dielectric anisotropy ε_a calculated as the difference in permittivity for $\mathbf{E}\|\mathbf{m}$ and $\mathbf{E}\perp\mathbf{m}$, is related to $\varepsilon_\|$ measured along $\mathbf{n}$ and $\varepsilon_\perp$ measured normally to $\mathbf{n}$ as $\varepsilon_a=2\varepsilon_\perp(\varepsilon_\perp-\varepsilon_\|)/(\varepsilon_\perp+\varepsilon_\|)$ [5]. Experimentally determined $\varepsilon_\|=9$ and $\varepsilon_\perp=6$ yield $\varepsilon_a=-2.4$ for a mixture with $P=0.48$ μm. Here and henceforth the numbers refer to the field frequency $\bar\omega=500$ Hz.

When $\varepsilon_a<0$, the vertical field $\mathbf{E}$ tends to reorient the layers vertically. Within the uniform domains, it causes Helfrich-Hurault undulation of layers with a threshold voltage U_{HH} that depends on h; $U_{HH}\sim\sqrt{h}$ [5]. For a mixture with $P=0.48$ μm, we measured $U_{HH}=12$ V for $h=5$ μm; $U_{HH}=17.5$ V at $h=10$ μm; $U_{HH}=20.3$ V at $h=15$ μm, and $U_{HH}=26.3$ V at $h=25$ μm. However, before undulations develop, one observes an instability of oily streaks (Fig. 1).

Field-controlled behavior of the oily streaks depends on their width. To distinguish basic scenarios, streaks in Fig. 1(a) are marked as #1 (narrow streaks; $2a<h$), #2 (intermediate streaks; $2a\approx h$), and #3 (wide streaks, $2a>h$). At $U=0$ V, a positive line tension keeps the streaks straight. As U slowly increases to some threshold $U_{th}=18$ V, the #2 streaks start to elongate, preserving the width [Fig. 1(b)]. The #1 and #3 streaks that are narrower or wider than #2 remain straight. If the ends of the #2 streak are pinned at spacers, then the streak extends by buckling. If the ends are not pinned, the #2 streak is pulled toward a #1 streak that is narrower. At $U>U_{th}$, the wide #3 streaks and some of the #1 streaks buckle as well [Fig. 1(c)]; however, the thinnest #1 streaks remain straight even above U_{HH}. Sometimes, a #1 streak is made wider by new curved layers propagating along its axis; when this happens, the streak buckles.

In the material we used, ε_a becomes positive above $\bar\omega\approx10$ kHz. The buckling instability occurs at all frequencies below 10 kHz. At $\bar\omega\approx10$ kHz, $\varepsilon_a=0$, no static instability is observed. At $\bar\omega>10$ kHz, the field stabilizes the planar texture; the streaks become thinner and disappear. Thus the field effect is predominantly dielectric (rather than, e.g., flexoelectric [5,6]). When $\varepsilon_a<0$, elongation of a streak substitutes an unfavorable state $\mathbf{m}\|\mathbf{E}$ outside the streak with a favorable tilted $\mathbf{m}$ inside the streak (Fig. 2). Nevertheless, the intuitive picture of dielectric response fails to describe the phenomenon even roughly; for example, the cause of different behavior of narrow and wide streaks remains unclear. In the model below the feature is explained if the standard dielectric and elastic terms are accompanied by the polar (''out-of-plane'') surface anchoring.

We start with the Lubensky–de Gennes coarse-grain theory [6] of a short-pitch cholesteric phase; in the experiment, $P\ll h$. The bulk free-energy density reads [6,7]

$$f_\nu=\tfrac{3}{16}K(\mathrm{div}\,\mathbf{m})^2+\tfrac{1}{2}Kq^2\delta^2-\tfrac{1}{2}\varepsilon_0\varepsilon_a E^2\cos^2\theta, \quad (1)$$
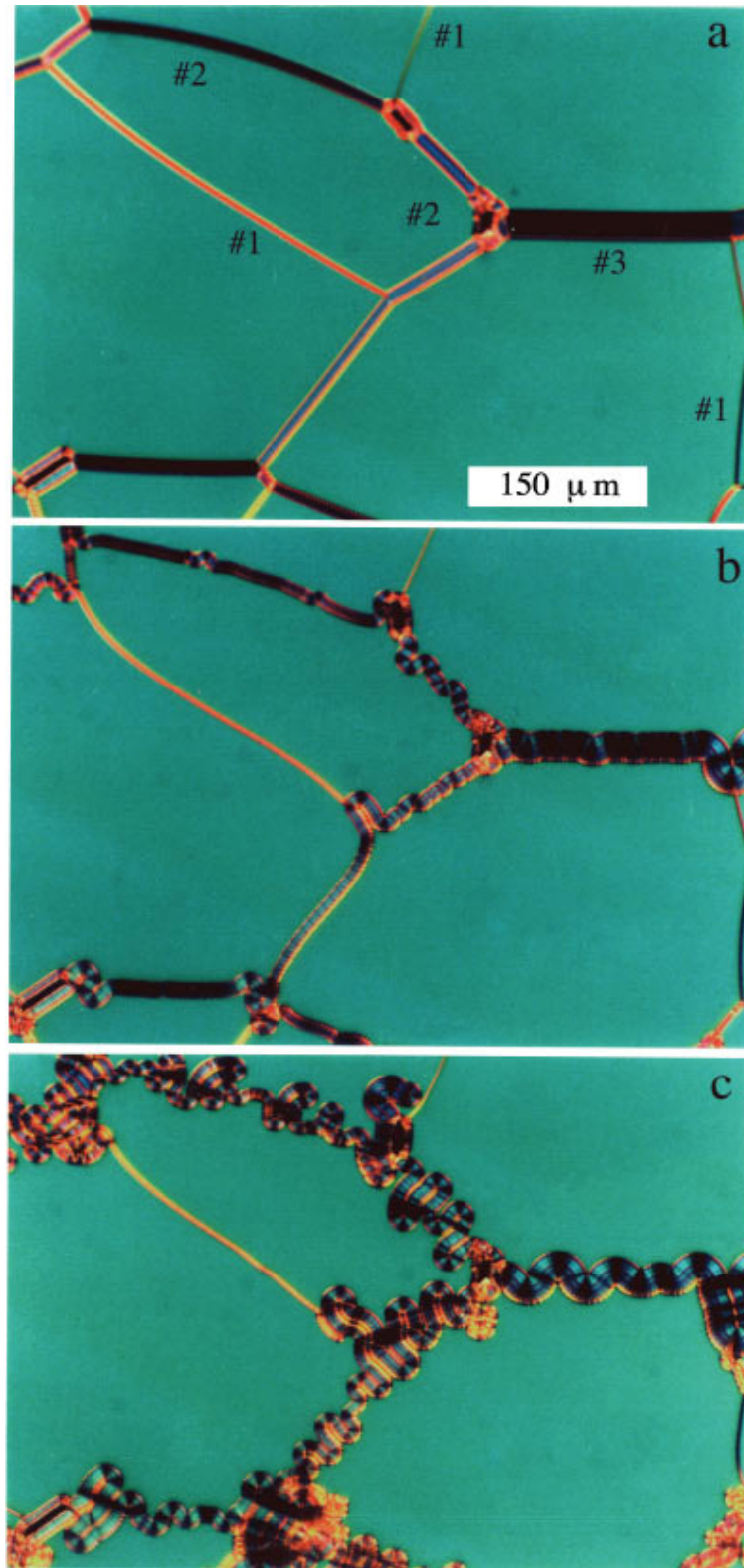
FIG. 1. (Color) Polarizing-microscope textures of oily streaks in a cholesteric sample ($P = 0.48$ μm, $h = 15$ μm, $\varepsilon_a = -2.4$) under applied voltage $U = 0$ V (a); 18.1 V (b); and 18.3 V (c). Oily streaks of different widths are marked #1 (width: $2 - 8$ μm); #2 ($12 - 18$ μm), and #3 (25 μm). The electric field is normal to the plane of the photographs.

where K is the bend elastic constant; Kq^2 is the compressibility modulus related to the change $\delta = P/P_0 - 1$ in the layers' thickness; $q = 2\pi/P$; ε_0 is the permittivity of vacuum; θ is the angle between $\mathbf{m}$ and the normal to the plates $\mathbf{k} \| \mathbf{E}$. The dielectric term in Eq. (1) is the cause of the instability; as E

increases, it becomes preferable to increase θ. The increase of θ is opposed by the elastic penalties [the first two terms in Eq. (1)] and by anchoring at the plates. So far, the anchoring properties of the cholesteric phase have been studied only for the free surface [8,9]. The consideration below refers to a
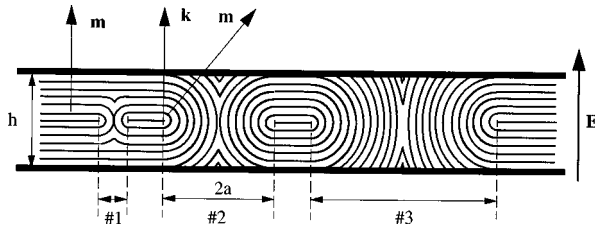
FIG. 2. Vertical cross section of three oily streaks of width $2a < h$ (#1), $2a \approx h$ (#2), and $2a > h$ (#3).

coarse-grain model and is thus similar to the models of "intrinsic" anchoring in the smectic-A phase [6,10,11].

At the surface, θ changes from $\theta = 0$ to $\theta = \arctan(2a/h)$. Tilted layers can match the tangential boundary conditions only if the helix is distorted, either continuously or through disclinations [8,9]. The anchoring energy is determined by the number $\sin|\theta|/P$ of layers crossing a horizontal plane, and by the energy $\sim K$ of each distorted zone or disclination:

$$f_s = w \ \sin|\theta| \big|_{z=0,h} , \tag{2}$$

where $w = \alpha K q$ is the anchoring coefficient and $\alpha \sim 1$ is a number defined by the geometry of distortions. Equation (2) is valid for small θ [6,10]. However, the amplitude of the potential (2), $w \sim \alpha K q$, is expected to be of the same order even when θ is large. Since we are interested in quantities integrated over θ, the particular choice of the angular dependence $f_s(\theta)$ does not matter much; in fact, the model predicts qualitatively the same results with a potential $f_s = w \ \sin^2 \theta$. In what follows, by integrating Eqs. (1) and (2) over the cross section of the oily streak, we calculate all relevant contributions to the line tension.

(i) The dielectric energy gain F_{diel}/K:

$$\frac{F_{\text{diel}}}{K} = -\frac{1}{\xi_E^2}\left[\xi - (1 + \xi^2)\arctan \xi + \frac{\pi}{2}\xi^2\right], \tag{3}$$

where $\xi_E = (2/Eh)\sqrt{(K/\varepsilon_0|\varepsilon_a|)}$ is the dimensionless dielectric length and $\xi = 2a/h$ is the dimensionless width of the streak.

(ii) The elastic energy of layer curvature:

$$\frac{F_{\text{el}}}{K} = \frac{3}{4}\left[\frac{\pi}{2}\ln\frac{\xi h}{2r_c} - \arctan \xi \ln \xi + L\left(\frac{\pi}{2} - \arctan \xi\right)\right.$$
$$\left. + L(\arctan \xi)\right], \tag{4}$$

where r_c is the core radius of the π disclinations and $L(x) = -\int_0^x \ln \cos t \, dt$ is the Lobachevski function [12]. The bend energy (4) should be supplemented by the core energy of linear and wall defects. The core energy of two disclinations scales as K per unit length; this small and constant correction is usually taken into account by a choice of r_c in Eq. (4) [4,6]. The energy (per unit area) of the wall can be estimated, following Ref. [4], as $f_w = (3K/4P)g(\theta)$, where $g(\theta)$ is some nonmonotonic function with a minima $g(\theta) = 0$ at $\theta = 0, \pi/2$ and maximum of the order of unity at $\theta = \pi/4$. We take $g(\theta) = \sin 2\theta$, which yields for the wall energy
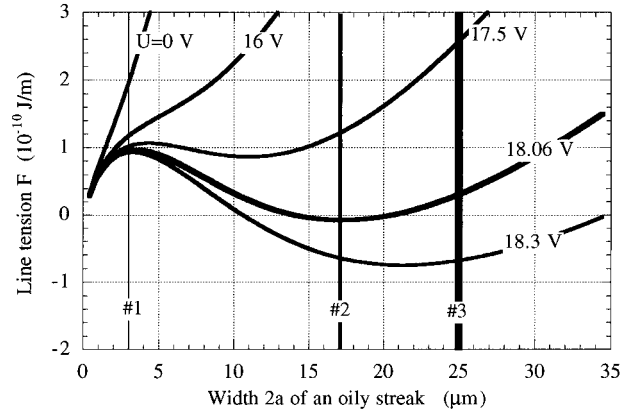

FIG. 3. Line tension F of the oily streak as a function of its width $2a$ and the applied voltage U as calculated from Eqs. (3)–(6). The vertical lines illustrate the behavior of narrow (#1), intermediate (#2), and wide (#3) oily streaks.

$$F_{\text{wall}}/K = (3\xi/4p) \ \ln(1 + \xi^{-2}); \tag{5}$$

$p = P/h$ is the renormalized pitch.

(iii) The surface anchoring penalty:

$$F_{\text{anch}}/K = (2/\xi_s) \ (\sqrt{\xi^2 + 1} - 1), \tag{6}$$

where $\xi_s = K/hw$ is the dimensionless anchoring extrapolation length.

Figure 3 shows how the total line tension $F = F_{\text{diel}} + F_{\text{el}} + F_{\text{anch}} + F_{\text{wall}}$ [Eqs. (3)–(6)] depends on the streak's width $2a$ and the voltage U. The parameters are the same as those in the experiment illustrated in Fig. 1: $h = 15 \ \mu\text{m}$, $P = r_c = 0.48 \ \mu\text{m}$, $K = 7 \times 10^{-12}N$, $\varepsilon_a = -2.4$. The only adjustable number is $\alpha = 1.4$ (which gives a reasonable $w \sim 10^{-4} \ \text{J/m}^2$). As an independent test, we used the values above to calculate the Helfrich-Hurault threshold $U_{\text{HH}}^2 = 2\sqrt{6}\pi^2 hK/\varepsilon_0|\varepsilon_a|P$ and compared it to the experimental U_{HH}. The two sets of U_{HH} differ by less than 10%.

Figure 3 gives a clear explanation of the observed phenomena. When the field is small, $F(2a)$ monotonically increases; the uniform defect-free state $2a = 0$ is at equilibrium. As U increases, $F(2a)$ becomes nonmonotonic; a local minimum appears at $2a \neq 0$ (see curve $U = 17.5$ V). This minimum is separated from the defect-free state by an energy barrier. At the threshold $U_{\text{th}} \approx 18.0$ V, the local minimum at $2a_{\text{th}} \neq 0$ becomes an absolute minimum. The line tension of the oily streak of width $2a_{\text{th}}$ turns negative. This streak can increase its length but there is no reason to increase the width; any $2a > 2a_{\text{th}}$ has a higher tension F. The feature is caused by the anchoring term and disappears when $w = 0$. At higher voltages, $U > 18.0$ V, the minimum gets deeper; streaks that are somehow wider or narrower than $2a_{\text{th}}$ acquire a negative tension too. However, the thinnest streaks retain their positive tension.

The in-plane buckling causes an additional energy penalty to fold the streak in the plane of the sample. This elastic energy is $\sim K \ln[R^2/(R^2 - a^2)]$; here R is the radius of curvature of the central wall. Taking $R = 2a$, one finds that the correction is small, $\sim 0.3 \ K \sim 10^{-12}N$.

The energy barrier in the dependencies $F(2a, U)$ reminds us of the classical picture of nucleation during a first-order

phase transition. An important difference brought about by anchoring, $w \neq 0$, is that the order parameter $\xi = 2a/h$, corresponding to the minimum of F, remains fixed at given $U > U_{th}$. As shown below, specific nonmonotonic behavior of $F(\xi)$ is caused by general trends in scaling with ξ rather than by a particular set of parameters in Fig. 3.

For $\xi \ll 1$ (narrow #1 streaks), expansion of $F(\xi)$ leads to

$$\frac{F}{K} = \frac{3\pi}{8} \ln \frac{\xi h}{r_c} + \frac{3}{2p} \xi \ln\left(\frac{1}{\xi}\right) + \left(\frac{1}{\xi_s} - \frac{\pi}{2\xi_E^2}\right)\xi^2 + O(\xi^3). \quad (7)$$

The first two elastic terms are positive and give rise to the energy barrier; the field term $\pi\xi^2/2\xi_E^2$ and anchoring term ξ^2/ξ_s are much smaller, since $\xi \ll 1$. In contrast, when $\xi \gg 1$ (wide #3 streaks), electric and anchoring terms scale as ξ and dominate, while the elastic terms become of little importance:

$$\frac{F}{K} = 2\left(\frac{1}{\xi_s} - \frac{1}{\xi_E^2}\right)\xi + \left(\frac{\pi}{2\xi_E^2} - \frac{2}{\xi_s} + \frac{3}{2}\pi \ln \frac{h}{r_c}\right) + O\left(\frac{1}{\xi}\right). \quad (8)$$

As a result, in the intermediate region $\xi_{th} \sim 1$ the dielectric term is capable of outbalancing both the anchoring and elastic energies to drive the line tension negative. At $\xi > \xi_{th}$ the anchoring penalty becomes larger than the dielectric gain.

Both experiment and numerical analysis of functions $F(\xi, U)$ suggest that the threshold voltage increases with h and decreases with P, approximately as $U_{th}^2 \sim h/P$ (Fig. 4). To get better insight into this result, we expand $F(\xi)$ in the vicinity of $\xi = 1$, $F = A_0 + A_1(\xi - 1) + \cdots$ and estimate U_{th}^2 from the condition $A_0 = 0$:

$$(\varepsilon_0\varepsilon_a/4) \, U_{th}^2 + 2wh(\sqrt{2} - 1) + (3Kh/4P) \ln 2 = 0 \quad (9)$$

[we drop the bend term which is $p^{-1} \ln p^{-1}$ times smaller than the wall energy $3Kh \ln 2/(4P)$]. Thus $U_{th}^2 \sim h/P$ if there is an intrinsic pitch-dependent anchoring $w \sim Kq$ that increases when the "layer thickness" P decreases; the wall energy alone does not allow a fit to the slope of the experimental dependencies U_{th}^2/h vs $1/P$ in Fig. 4. Usually, field effects in cholesteric cells are described without a specific anchoring term, with the assumption that either $w \to \infty$ (Helfrich-Hurault undulations [5,6], buckling of Cano dislo-
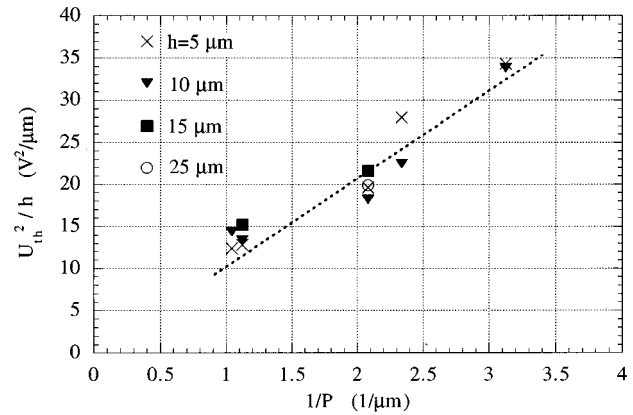

FIG. 4. Experimental and theoretical (dashed line) dependencies U_{th}^2/h vs $1/P$.

cations in a magnetic field [6,13,14]) or $w = 0$ (field-induced unwinding of a cholesteric helix [6]). On the other hand, there are effects of current interest, such as electrical switching of polymer-stabilized cholesteric displays [15] or diffraction gratings [16] where the issue of anchoring must be addressed. Equation (9) predicts also that U_{th} can be smaller than U_{HH}; with $w = \alpha Kq$ and $\alpha = 1.4$, one finds that $U_{th}^2/U_{HH}^2 \approx 0.7$, in agreement with experiment.

Buckling instabilities of domain walls have been observed in other systems such as magnetic films [17] and monolayers [18]. In these media, the walls are of equal width and one cannot control the line tension selectively. Thus the cholesteric system can be used to study the dynamics of cellular networks by controlling the net force at the vertices where different streaks meet. Elimination of oily streaks by field when $\varepsilon_a > 0$ is another interesting subject to study, since it results in a defect-free planar state. Further work is required to describe the director configurations in the bulk and at the surface. The coarse-grain model neglects director distortions within the curved layers. However, these distortions become important when one addresses questions about the shape of buckling streaks, the interaction of closely located streaks, or the relation between "intrinsic anchoring" $w \sim Kq$ and normal anchoring of the director at the cholesteric interface.

[1] D. Weaire and N. Rivier, Contemp. Phys. **25**, 59 (1984).
[2] O. Lehmann, Z. Phys. Chem., Stoechiom. Verwandtschaftsl. **4**, 462 (1889); F. Reinitzer, Ann. Phys. (Leipzig) **27**, 213 (1908).
[3] G. Friedel, Ann. Phys. (Paris) **18**, 273 (1922).
[4] M. Kléman, *Points, Lines and Walls* (Wiley, New York, 1983).
[5] L. M. Blinov and V. G. Chigrinov, *Electrooptic Effects in Liquid Crystal Materials* (Springer-Verlag, New York, 1994).
[6] P. G. de Gennes and J. Prost, *The Physics of Liquid Crystals* (Clarendon, Oxford, 1993).
[7] Since $|\varepsilon_a| < \varepsilon_\parallel, \varepsilon_\perp$, we neglect the effects of the field nonhomogeneity in the cell.
[8] P. E. Cladis and M. Kléman, Mol. Cryst. Liq. Cryst. **16**, 1 (1972).
[9] R. Meister, H. Dumoulin, M.-A. Hallé, and P. Pieranski, J. Phys. II **6**, 827 (1996).
[10] G. Durand, Liq. Cryst. **14**, 159 (1993).
[11] Z. Li and O. D. Lavrentovich, Phys. Rev. Lett. **73**, 280 (1994).
[12] I. S. Gradshteyn and I. M. Ryzhik, *Tables of Integrals, Series, and Products* (Academic, New York, 1980).
[13] Orsay Liquid Crystal Group, Phys. Lett. A **28**, 687 (1969).
[14] M. Kléman and J. Friedel, J. Phys. (France) **30**, C4-43 (1969).
[15] D.-K. Yang, J. L. West, L.-C. Chien, and J. W. Doane, J. Appl. Phys. **76**, 1331 (1994).
[16] D. Subacius, S. V. Shiyanovskii, Ph. Bos, and O. D. Lavrentovich, Appl. Phys. Lett. **71**, 3323 (1997).
[17] K. L. Babcock and R. M. Westervelt, Phys. Rev. A **40**, 2022 (1989).
[18] K. J. Stine, C. M. Knobler, and R. C. Desai, Phys. Rev. Lett. **65**, 1004 (1990).